SPH Simulation of Ship Behaviour in Severe Water-Shipping Situations

Kouki Kawamura, *National Maritime Research Institute*, kawamura@nmri.go.jp

Hirotada Hashimoto, *Kobe University,* hashimoto@port.kobe-u.ac.jp

Akihiko Matsuda, *National Research Institute of Fisheries Engineering,* amatsuda@fra.affrc.go.jp

Daisuke Terada, *National Research Institute of Fisheries Engineering*, dterada@fra.affrc.go.jp

ABSTRACT

Fishing vessels, having relatively small freeboard, are prone to suffer water-shipping in severe sea state. The water impact and the accumulated water effect could make fishing vessels be unstable and capsize in the worst situation. Therefore to secure the safety of fishing vessel under water-shipping condition is important, but it is not easy to numerically predict the water behaviour/influence associated with the violent water-shipping where the water impact, the large free-surface deformation, and the strong coupling with the ship motion appear compositely. In this paper, SPH simulation using GPU is performed to predict the 6DoF ship motion in water-shipping situations. Then the prediction accuracy of the SPH method is investigated through comparisons with dedicated captive and free-motion tests.

Keywords: *Water-shipping, SPH, 6DoF motion, Experiment, GPU*

1. INTRODUCTION

Since most of Japanese fishing vessels have relatively small freeboard to increase the efficiency of fishery operation/fishery regulation using gross tonnage, they occasionally suffer water-shipping in severe sea state. The shipped water is easily accumulated on deck because of the existence of large bulwark, so the water-shipping event has potential danger resulting in large heeling/capsizing in the worst situation. Since there have been many accident reports in which fishing vessels capsized due to most likely the water-shipping, there is a strong demand to develop a numerical simulation method for ship dynamic behaviours when suffering serious water-shipping. However, water-shipping problems contain several difficulties; how to deal highly nonlinear free-surface flows and their impacts and to estimate the coupling effect with ship motions. Therefore, advanced numerical approaches are required for the quantitative assessment of ship stability/safety against the severe water-shipping. Analytical approaches are very limited for this event because the nonlinear free-surface flows are to be dealt, and CFD (Computational Fluid Dynamics) has good ability to overcome the difficulties. Among CFDs, mesh-based CFD is well developed and evaluated so far but still have difficulties/complexity to precisely capture the largely-deformed free surface flows with the fragmentation and the reconnection, and particle methods have an advantage in terms of the capturing of non-diffusive nonlinear free-surface flows.

In this paper, the SPH (Smoothed Particle Hydrodynamics) method, which is a truly mesh-free CFD and is fully Lagrangian method, is applied to a water-shipping problem. In order to investigate the applicability of the SPH method, a captive model test in steep waves is firstly conducted to observe the water on deck situation and to measure the hydrodynamic force acting on the ship model in water-shipping condition. Then the SPH result is compared with the experiment to confirm the prediction accuracy. Secondly ship motion measurement in steep wave trains is executed for the same ship model. Then a SPH simulation of 6DoF (Degrees of Freedom) motions, including the water-shipping event in in regular steep waves, is executed and compared with the measurement. Through the comparisons with the captive and free-motion tests, it is demonstrated that the SPH method provides a promising result for realizing the quantitative safety assessment of fishing vessels in severe water-shipping condition.

2. NUMERICAL METHOD

SPH

The SPH method derives from astrophysical field and was developed by Monaghan (1994) for free-surface flows of weak-compressible fluid. The SPH governing equations dealing with compressible fluids are shown in Eqs.1-2. The momentum conservation equation can be written in SPH notation as Eq.3 and the viscous term Π_{ij} is calculated using the artificial viscosity proposed by Monaghan (1992) given as Eqs.4-5. The pressure of weakly compressible fluid is determined by solving an equation of state expressed as Eq.6 (Monagan and Kos, 1999). The quintic form kernel (Wendland, 1995), Eq.7, is used as the SPH interpolator. Time forwarding is explicit for all equations, so the SPH method is suitable for parallel computing using GPU (Graphics Processing Unit). Further explanation and references can be found in literatures, e.g. SPHysics user guid by Gesteira et al. (2010).

$$\frac{D\rho}{Dt} + \rho\nabla\cdot\boldsymbol{u} = 0 \tag{1}$$

$$\frac{D\boldsymbol{u}}{Dt} = -\frac{1}{\rho}\nabla P + \boldsymbol{g} + \boldsymbol{\Theta} \tag{2}$$

$$\frac{d\boldsymbol{u}}{dt} = -\sum_j m_j \left(\frac{P_j^2}{\rho_j^2} + \frac{P_i^2}{\rho_i^2} + \Pi_{ij} \right) \nabla_i W_{ij} + \boldsymbol{g} \tag{3}$$

$$\Pi_{ij} = \begin{cases} \dfrac{-\alpha c \mu_{ij}}{\rho} & u_{ij} r i_j < 0 \\ 0 & u_{ij} r i_j > 0 \end{cases} \tag{4}$$

$$\mu_{ij} = \frac{h\boldsymbol{u}_{ij}\boldsymbol{r}_{ij}}{\boldsymbol{r}_{ij}^{\ 2} + (0.01h^2)^2} \tag{5}$$

$$P = \frac{c_0^{\ 2}\rho_0}{7}\left[\left(\frac{\rho}{\rho_0} \right)^7 - 1 \right] \tag{6}$$

$$W(r,h) = \frac{21}{16\pi h^3}\left(1 - \frac{q}{2}\right)^4 (2q+1) \qquad 0 \le q(=r/h) \le 2 \tag{7}$$

SPH solver

An open source code of DualSPHysics (http://dual.sphysics.org/) that combines CUDA and OpenMP, based on the SPH method is used. DualSPHysics can utilise GPUs for arithmetic processing, so that over 3,000 threads parallelization can be performed on CUDA platform. Because of difficulties in implementation of several algorithms into GPU-based code, the basic SPH algorithms, not the latest ones, are available in the current DualSPHysics code. However DualSPHysics can deal with much large number of particles as compared to the ParallelSPH code, so that the global analysis of ship motions, incident waves and their interactions as well as the local water-shipping phenomenon can be solved in the same framework.

In this study, TeslaC2050 developed for GPU computing and GTXTITAN done for gaming are used. The numerical models and conditions used for the SPH simulation are shown in Table 1. The reduced speed of sound is used to avoid the excessive CPU load and is decided not to exceed the certain Mach number. The variable time step is determined to satisfy the CFL (Courant-Friedrichs-Lewy) condition in each step.

Table 1 Numerical condition

Time step marching	Verlet
Viscosity parameter: α	0.08
Kernel compact support: $2h$ [m]	0.225
Speed of sound: C [m/s]	26.7
Particle distance: dx [m]	0.075
CFL number	0.3

3. MODEL EXPERIMENT

In order to investigate the applicability/accuracy of the SPH method for water-shipping problems, a model experiment for validation is conducted. The model ship is an 80 tonnage Japanese purse seiner because she could suffer the water-shipping in stormy wave condition due to the relatively small freeboard. As a first step towards quantitative safety assessment of the fishing vessel against the water on deck, a simplified ship model, in which the ship profile along the centre line is uniformly projected in width direction, is used as shown in Fig.1. The principal dimension of the model is shown in Table 2. The heights of freeboard and forecastle, L/B, and L/D are set to keep the original value of the subject fishing vessel. For the simplicity, the bulwark is neglected in this study.

With use of the simplified ship model, a captive test and free-motion measurement are conducted to validate the SPH simulation using a GPU.

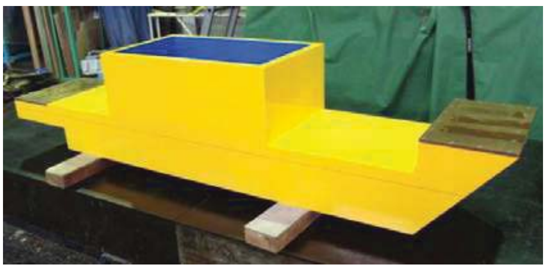

Figure 1 Simplified purse-seiner model

Table 2 Particulars of the model

Length : L_{OA} [m]	1.6
Breadth : B [m]	0.33
Depth : D [m]	0.126
Draught: d [m]	0.12
mass : M [kg]	55.2
Metacentric height: GM [m]	0.00922
Gyro radius in roll: k_{xx}/B	0.40
Gyro radius in pitch: k_{yy}/L	0.30
Gyro radius in yaw: k_{zz}/L	0.30

Captive test

A captive model experiment is conducted at the towing tank of Osaka University. The ship model is fixed in 6 degrees of freedom, and hydrodynamic forces of surge, sway, roll and yaw are measured by a dynamometer located at the centre of ship gravity. Regular wave trains are generated by a plunger-type wave generator. The wave condition used in the captive test is shown in Table 3. The encounter angle to the incident waves is set to be zero (following wave) and sixty (stern quartering wave) degrees.

Table 3 Wave condition

λ [m]	H [m]	H/λ	λ/L
1.75	0.1575	0.090	1.094

Free-motion test

Ship motion measurement is conducted at the seakeeping and manoeuvring basin of National Maritime Research Institute of Fisheries Engineering. The ship model is completely free in the experiment and all the 6 DoF component of surge, sway, heave, roll, pitch, and yaw are measured by an on-board optical gyro scope and a total station system, and are stored in an on-board computer. The instantaneous position of the centre of ship gravity in the earth-fixed coordinate system can be measured by the total station system. (Umeda et al., 2014) The total station system uses two prisms attached to the ship model with the different position. The theodolite emits light to the prisms and measures the phases of lights reflected by the prisms, so the instantaneous position of each prism in the earth-fixed coordinate can be calculated. By combining the positions of the two prisms and roll, yaw, and pitch angles measured by the gyro scope, instantaneous position of the centre of ship gravity can be determined. The prisms and the theodolite used in the experiment are shown in Fig.2.

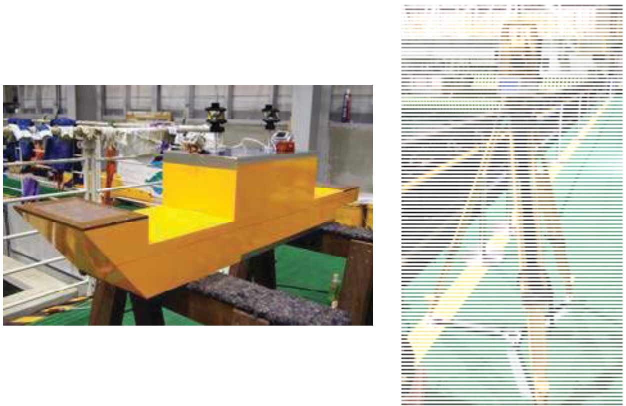

Figure 2 Two prisms (left) and theodolite (right)

Regular steep waves are generated by a plunger-type wave generator and the tested wave condition is shown in Table 4. The initial encounter angle to the wave is 0 degrees (following wave). Firstly a vertical motion is excited by wave-ship interaction and a lateral motion is also excited after a while, and then the fully combined 6 DoF motion is excited. During the measurement, the shipping water on both the fore and aft upper decks is recorded by a water-proof camera of GoPro hero3.

Table 4 Wave condition

λ [m]	H [m]	H/λ	λ/L
1.75	0.1945	0.111	1.094

4. RESULTS AND DISCUSSION

Numerical simulations using the DualSPHysics code are performed for the same conditions as the captive test and free-motion measurement to discuss the applicability/accuracy of the SPH method in the prediction of 6 DoF motions under water-shipping situations. Regular waves are generated by a flap-type wave generator realized by imposing the moving wall boundary condition.

Captive test

In the simulation of captive test, different sizes of numerical wave tanks are used depending on the encounter angle to reduce CPU costs as shown in Table 5. The comparisons of hydrodynamic force acting on the ship between the experiment and the SPH simulation are shown in Figs.3-4. Here t=0 means the time when a wave crest is passing the centre of ship gravity. Figs.5-6 show the water-shipping situation.

Table 5 Numerical wave tank

<table>
<tr><td>Encounter angle [deg]</td><td>Length [m]</td><td>Width [m]</td><td>Depth [m]</td></tr>
<tr><td rowspan="3">0.0</td><td>7.5</td><td>1.5</td><td>1.2</td></tr>
<tr><td>No. of fluid particles [million]</td><td>No. of wall particles [million]</td><td>Total No. of particles [million]</td></tr>
<tr><td>12.30</td><td>1.37</td><td>13.67</td></tr>
<tr><td>Encounter angle [deg]</td><td>Length [m]</td><td>Width [m]</td><td>Depth [m]</td></tr>
<tr><td rowspan="3">-60.0</td><td>7.5</td><td>3.0</td><td>1.2</td></tr>
<tr><td>No. of fluid particles [million]</td><td>No. of wall particles [million]</td><td>Total No. of particles [million]</td></tr>
<tr><td>25.18</td><td>1.76</td><td>26.94</td></tr>
</table>

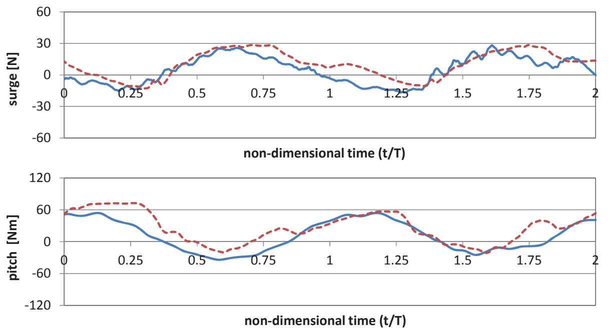

Figure 3 Comparison of wave-induced surge force and pitch moment (χ=0deg)

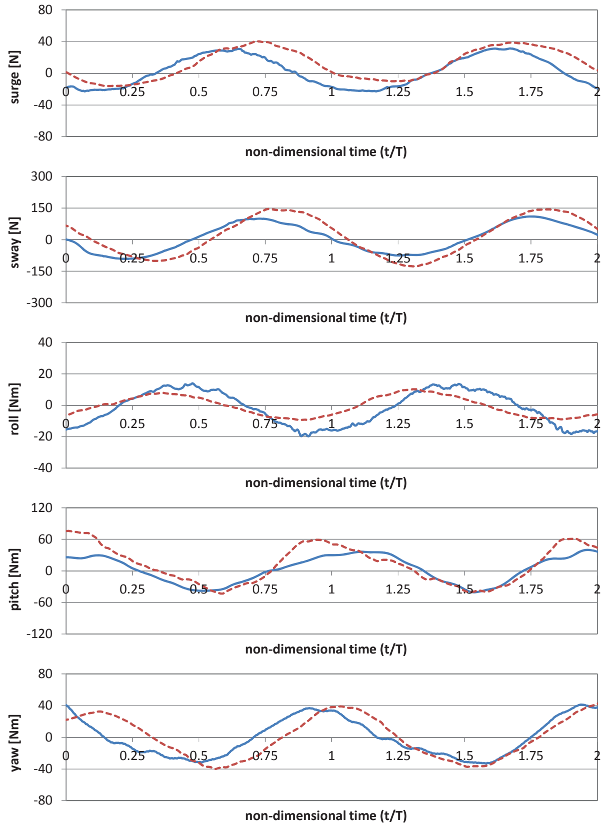

Figure 4 Comparison of wave-induced surge force and pitch moment (χ=60deg)

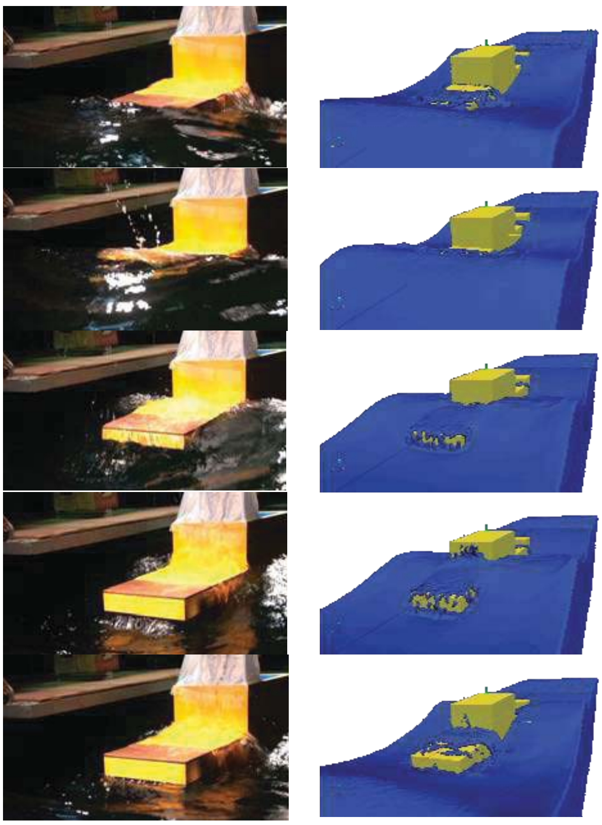

Figure 5 Comparison of water-shipping situation (χ=0deg)

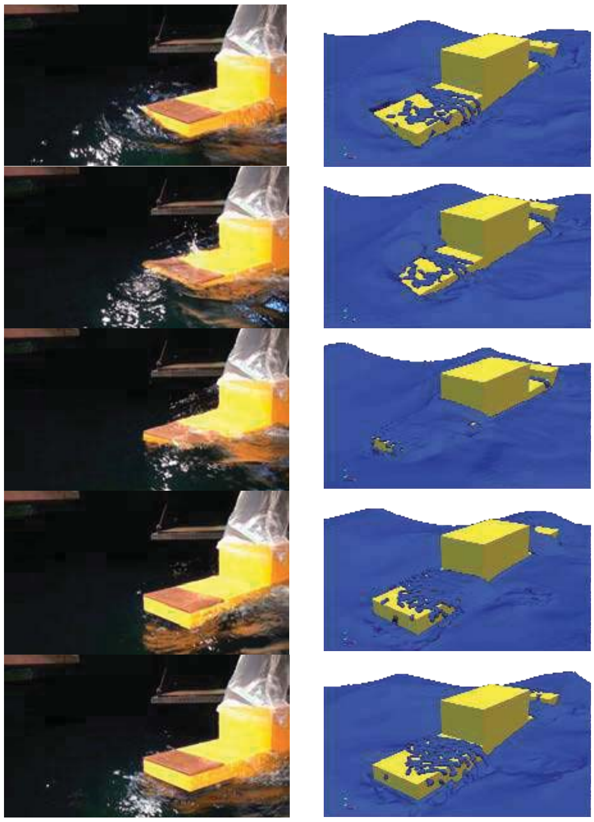

Figure 6 Comparison of water-shipping situation (χ= -60deg)

In case of the encounter angle of 0 degrees, the hydrodynamic force in heave and pitch becomes vertically asymmetric. This phenomenon can be explained that the water impact to the superstructure push the ship forward as well as the steady drift force in surge and the accumulated water on the aft deck induce the bow-up moment in pitch, under severe water-shipping situation. The SPH method can capture this experimentally confirmed trend. In case of the encounter angle of 60 degrees, the asymmetric pitch disappears because the water on deck happens not only on the aft deck but also on the fore deck. The amplitude of wave-induced yaw moment is well predicted by the SPH simulation but there is certain phase shift, and the prediction accuracy is not so satisfactory in sway and roll. This discrepancy might be improved by increasing the number of fluid particles, which equals to increase the spatial resolution, because the pressure assessment for thin layer of shipping water requires a certain number of particles in vertical direction.

4.2 Free-motion test

The SPH simulation with the same condition of the ship motion measurement is executed. The size of numerical tank, the numbers of fluid and wall particles are shown in Table 6, respectively. Numerical test is performed with the initial angles of -3 degrees and 60 degrees for the comparison of transient and steady motions, respectively. The comparisons of the x- and y-positions, heave, roll, pitch and yaw motions between the model experiment and the SPH simulation are shown in Figs.7-8.

Table 6 Numerical wave tank

Length [m]	Width [m]	Depth [m]
10.0	3.0	0.5
No. of fluid particles [million]	No. of wall particles [million]	Total No. of particles [million]
23.22	1.34	24.56

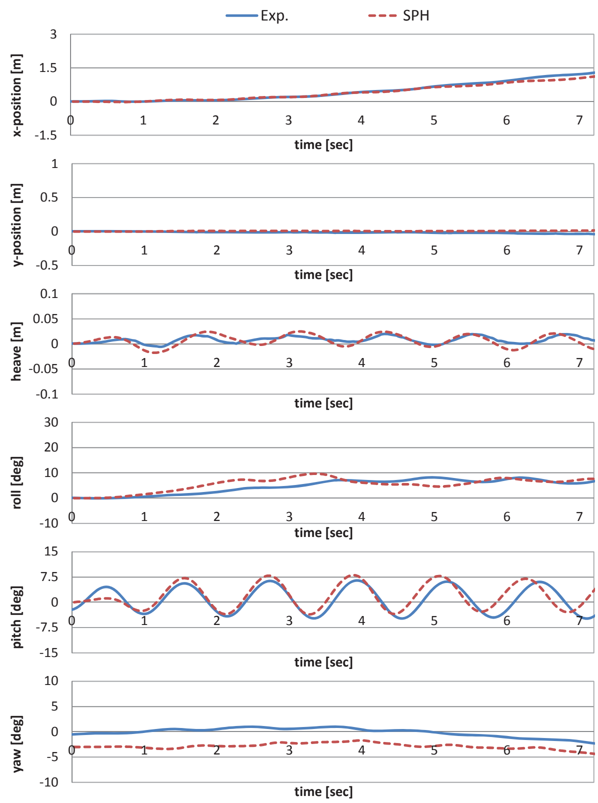

Figure 7 Comparison of transient motion in following waves

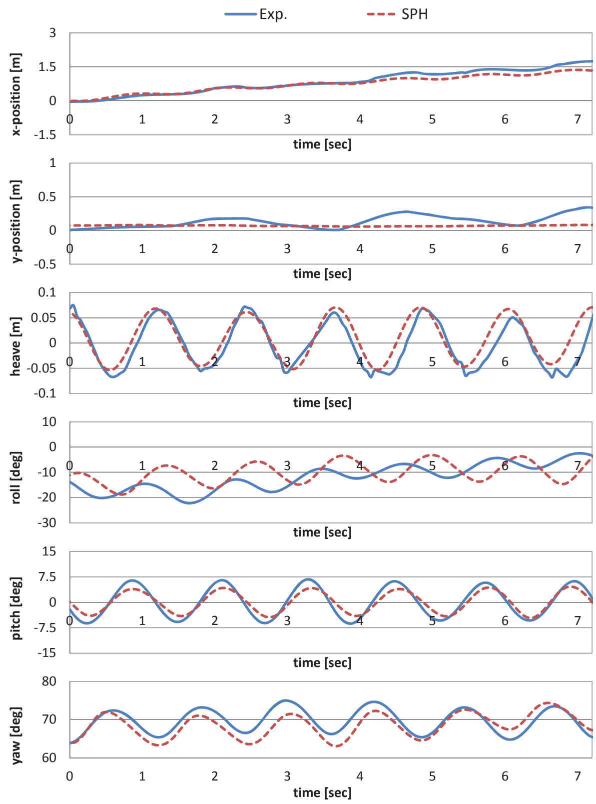

Figure 8 Comparison of steady periodic motion in stern quartering waves

Both in the experimental and numerical results for a transient motion, the lateral motions are almost negligible because of the small encounter angle, except for the heeling due to accumulated water on deck. The drift in longitudinal-direction (surge), heave and pitch motions are dominant in this situation, and the SPH well reproduces the experimental result. In case of a periodic steady state, the SPH result agrees with the experimental one qualitatively in all the 6 DoF motions. The agreement in sway and roll motions are slightly worse than other 4 motions, as presumed from Fig.4. The numerical simulation of the ship motion in steep waves shows the consistent result with the captive test results. To summarize, the prediction accuracy of the ship behaviour in severe water-shipping condition is reasonable and acceptable for practical uses.

Comparisons of the ship behaviour and the shipping water situation on the aft deck are shown in Figs.9-10 and Figs.11-12, respectively. In the experimental result of the transient motion, severe water-shipping on the aft deck happens and hits the vertical wall of the superstructure with the significant water splashing. The SPH result well reproduces the ship-wave interaction with the violent shipping water flows in following seas. In the periodic steady state, the water-shipping happens much less compared to the transient motion both in the experiment and the simulation. Regarding the water on deck situation, the experimental result is more violent in the transient motion and the amount of the water on deck is larger in the steady state than the SPH results. For the first discrepancy, it might be because that water flows tend to over-damp due to the energy dissipation when the artificial viscosity is used. For the second discrepancy, the predicted amplitude of pitch moment is smaller than the experiment as shown in Fig.8, so the amount of water on deck becomes smaller because the water-shipping mainly happens when the ship stern is going down.

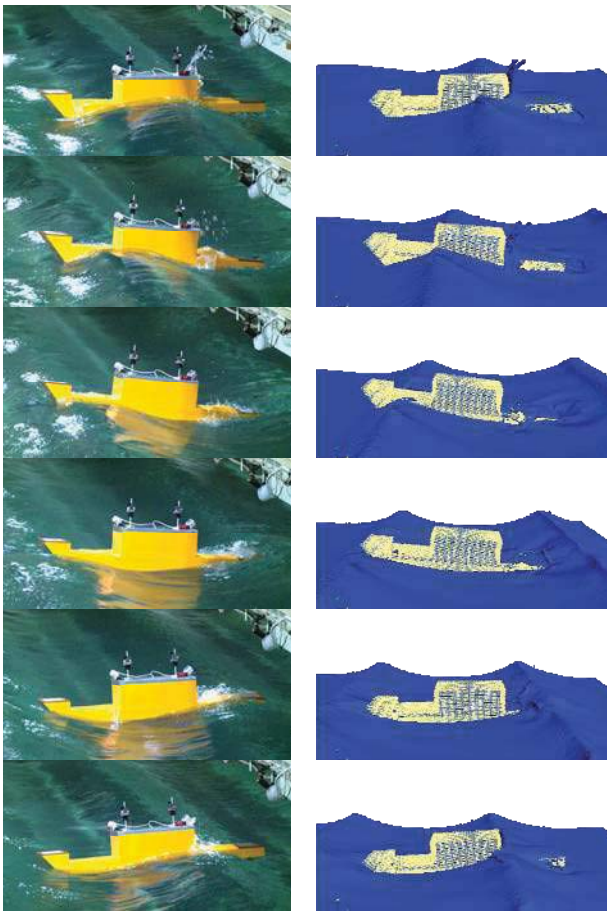

Figure 9 Comparison of ship transient motion

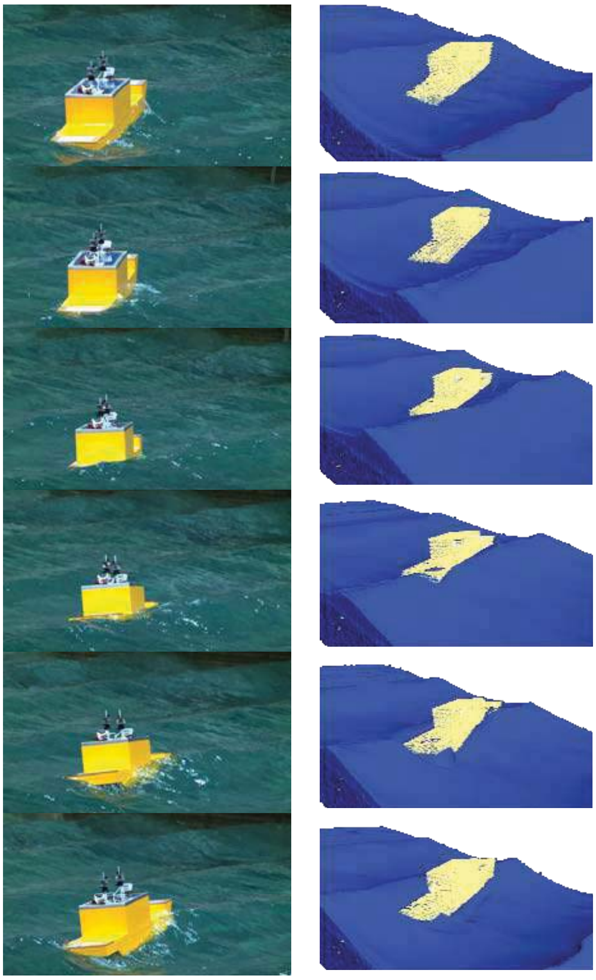

Figure 10 Comparison of ship steady motion

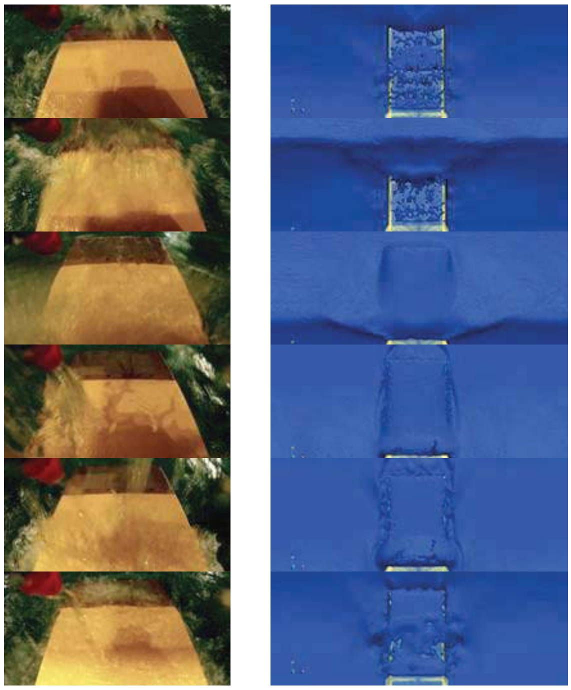

Figure 11 Comparison of shipping water on the aft deck in transient state

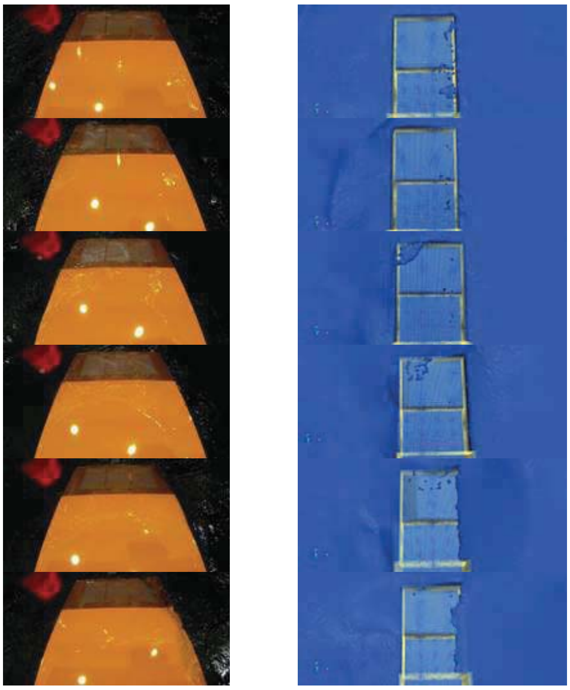

Figure 12 Comparison of shipping water on the aft deck in steady state

5. CONCLUSIONS

SPH simulation using GPU is performed to predict the 6DoF ship motion in water-shipping condition. The applicability and the prediction accuracy are investigated through comparisons with dedicated captive and free-motion tests in very steep waves using a simplified model of a fishing vessel. The calculated wave-induced hydrodynamic force agrees with the captive test qualitatively and the SPH method well reproduces the ship dynamic behaviour, in severe water-shipping situations. From the comparison results, it is demonstrated that the SPH simulation using GPU has good potential for the quantitative safety assessment of fishing vessels in water-shipping situation. Similar investigation using more realistic 3-D hull geometries is expected as a next step.

6. ACKNOWLEDGMENTS

This work was supported by JSPS KAKENHI Grant Number 26630454.

7. REFERENCES

Gesteira, M.G., Rogers, B.D., Dalrymple, R.A., Crespo, A.J.C. and Narayanaswamy, M., 2010, "User Guide for the SPHysics code", https://wiki.manchester.ac.uk/sphysics/index.php/Documentation

Monaghan, J.J., 1992, "Smoothed particle hydrodynamics", Annual Rev. Astron. Appl., 30: pp. 543-574.

Monaghan, J.J., 1994, "Simulating free surface flows with SPH", Journal Computational Physics, 110: pp. 543-574.

Monaghan, J.J. and Kos, A., 1999, "Solitary waves on a Cretan beach", J. Wtrwy. Port, Coastal and Ocean Eng., 125: pp. 145-154.

Umeda, N., Furukawa, T., Matsuda, A. and Usada, S., 2014, "Rudder Normal Force during Broaching of a Ship in Stern Quartering Waves", Proceedings of the 30th Symposium on Naval Hydrodynamics, Tasmania.

Wendland, H., 1995, "Piecewise polynomial, positive definite and compactly supported radial functions of minimal degree", Advances in Computational Mathematics, 4(1): pp. 389-396.

8. NOMENCLATURES

ρ	density
t	time
$\boldsymbol{u}$	velocity vector
P	pressure
$\boldsymbol{g}$	gravity vector
$\boldsymbol{\Theta}$	diffusion term
m	mass
W	weight function
α	tuning parameter
c	speed of sound
$\boldsymbol{r}$	position vector
λ	wave length
H	wave height